

# MODEL-BASED KLYSTRON LINEARIZATION IN THE SWISSFEL TEST FACILITY

Amin Rezaeizadeh\*, Paul Scherrer Institut, Villigen, Switzerland  
 and Automatic Control Laboratory, ETH, Zürich, Switzerland  
 Roger Kalt, Thomas Schilcher, Paul Scherrer Institut, Villigen, Switzerland  
 Roy Smith, Automatic Control Laboratory, ETH, Zürich, Switzerland

## Abstract

An automatic procedure is developed to provide the optimal operating point of a klystron. Since klystrons are non-linear with respect to the input amplitude, a model-based amplitude controller is introduced which uses the klystron characteristic curves to obtain the appropriate high voltage power supply setting and amplitude, such that the operating point is close to the saturation. An advantage of the proposed design is that the overall open-loop system (from the input to the RF station to the klystron output amplitude) is linearized. The method has been successfully tested on a full scale RF system running at nominal power.

## INTRODUCTION

The Swiss Free Electron Laser is currently being constructed at PSI [1]. The SwissFEL injector and the Linac Radio Frequency drives operate in a pulsed mode at the rate of 100 Hz. The pulse-to-pulse stability of the electron beam characteristics, such as beam energy, are crucial for the quality of laser pulses. As the RF phase and amplitude stability plays a significant role in this goal, an automatic procedure is developed to obtain the operating point of a klystron such that the output amplitude is close to its saturation level so that the pulse-to-pulse amplitude jitter is minimized. The procedure is model-based, using the klystron (AM/AM) characteristic curves. The major advantage of the design is that the overall system from the Low Level RF input to the vector modulator to the output of the klystron is linearized. Moreover, from the system dynamics standpoint, the closed-loop system can be treated as a linear system. A recent contribution [2], uses a third order polynomial function to correct the nonlinearity of the klystron. The method is open-loop and for constant high voltage.

Throughout this paper, the klystron and the upstream RF and LLRF subsystems such as the pre-amplifier and the vector modulator are referred to as the “drive chain”. The high voltage power supply setting and the input amplitude to the klystron are automatically determined according to the desired output power and the predefined headroom to the saturation. For the case where the demand power is obtainable via slight change in the input amplitude, the high voltage is kept unchanged. For precise control, a pulse-to-pulse feedback loop is closed around the operating point.

In the following section, we discuss the klystron amplitude-to-amplitude (AM/AM) modeling, followed by a pulse-to-pulse amplitude feedback scheme.

## KLYSTRON MODELING

For fixed and constant high voltage, the klystron can be characterized by Rapp’s model used for solid-state power amplifiers (SSPA) [3] (which was initially introduced by Cann in 1980 [4]). The model is suitable for systems that are approximately linear with gradual saturation. We generalize the formulation of the model as follows,

$$y(a_{in}) = \frac{p_1 a_{in} + p_2}{\sqrt{1 + \left(\frac{a_{in}}{p_0}\right)^2}} + p_3, \quad (1)$$

where,  $y$  denotes the output amplitude of the klystron,  $a_{in}$  is the input amplitude and  $p_i$ ’s are constant parameters. This model describes the saturation and over-saturation characteristics of a klystron for constant high voltage.

Figure 1 illustrates the data of a klystron in the SwissFEL test facility and the fitted model from (1). In the original form [3, 4], the  $p_2$  term is zero which does not capture the power drop in the over-saturation region.

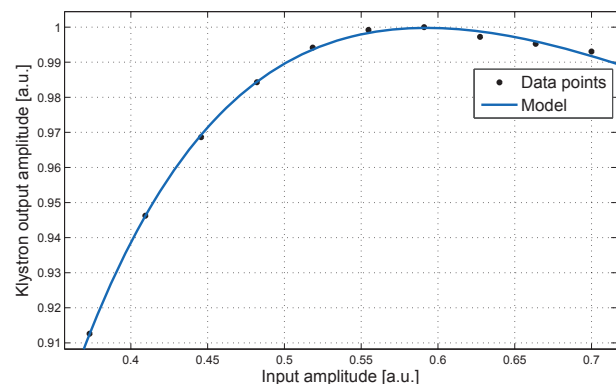


Figure 1: The klystron input-amplitude to output-amplitude (AM/AM) conversion curve. The output amplitude is normalized to the maximum amplitude. The regression of fitting is  $R^2 = 0.999$ .

According to the experiments, the output amplitude change is approximately linear with respect to high voltage changes. Therefore, the following formulation is introduced, connecting the input, output amplitude and the high voltage

\* aminre@ee.ethz.ch

value.

$$y = f(a_{in}, h) := \frac{p_1 a_{in} + p_2 h + p_3 a_{in} h + p_4}{\sqrt{1 + (\frac{a_{in}}{p_0})^2}} + p_5 h + p_6, \quad (2)$$

where  $y$  is the output amplitude,  $h$  denotes the high voltage power supply value, and  $p_i$ 's are constant parameters. Figure 2 shows the characteristic curves of the same klystron for different high voltage levels of  $h$ . The fitted curves are plotted in red. The output power,  $P$ , is directly calculated from (2) by squaring the output amplitude and multiplying by a power factor.

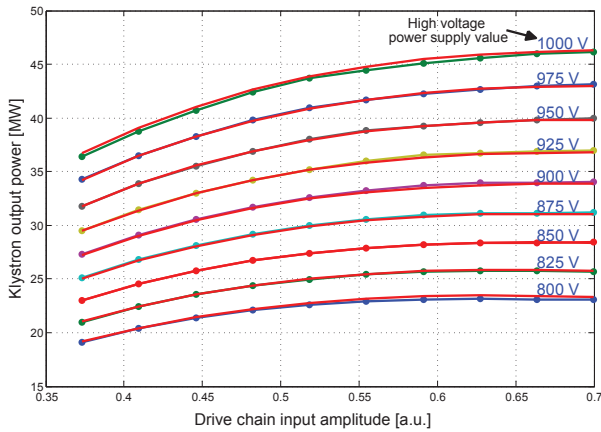


Figure 2: The klystron output power,  $P$ , for different input amplitudes and high voltage power supply levels,  $h$  (numbers in blue). The models are depicted in red. The fitting regression is  $R^2 = 0.9996$ . The standard deviation of the error between the fit and the data for the saturating powers is  $\sigma \approx 0.19 MW$  which corresponds to 0.65% headroom.

### OPERATING POINT DETERMINATION

The operating point of the klystron is defined by the output power,  $P^*$ , the high voltage power supply setting,  $h^*$ , and the drive chain input amplitude,  $a_{in}^*$  (see Fig. 3).

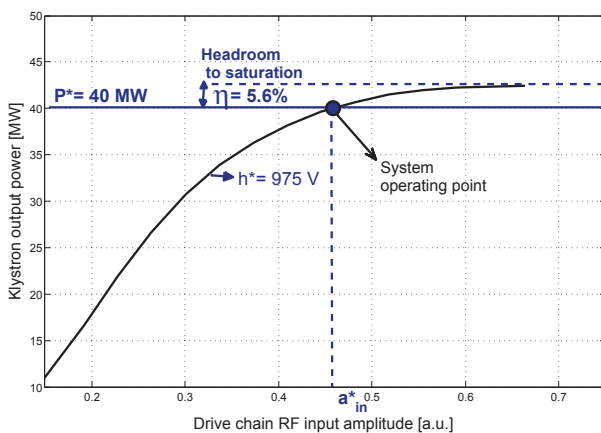


Figure 3: The operating point definition of the klystron.

For output amplitude stability (repeatability), it is preferable to operate the klystron very close to its saturation. The amount of the headroom to saturation level is given in percent and it is normally around 1 to 5 %. The maximum output amplitude,  $y_{max}$ , can be readily determined from (2):

$$y_{max} = \sqrt{(p_2 h + p_4)^2 + p_0^2 (p_3 h + p_1)^2} + p_5 h + p_6. \quad (3)$$

Since the desired headroom is specified, the desired output amplitude can be expressed in terms of  $y_{max}$ ,

$$y^* = (1 - \eta) y_{max}, \quad (4)$$

where  $y^*$  is the desired output amplitude which corresponds to  $P^*$ , and where  $\eta$  denotes the headroom.

From Eqs. 3 and 4, the corresponding setpoint value for high voltage power supply,  $h^*$ , can be easily calculated. In practice, equation (3) is close to linear with respect to the high voltage power supply,  $h$ .

Once  $h^*$  is determined, the calculation of the corresponding input amplitude,  $a_{in}^*$ , is straightforward. Substituting  $h^*$  and  $y^*$  into the model defined in (2), leads to,

$$y^* = \frac{p_1 a_{in}^* + p_2 h^* + p_3 a_{in}^* h^* + p_4}{\sqrt{1 + (\frac{a_{in}^*}{p_0})^2}} + p_5 h^* + p_6. \quad (5)$$

Equation 5 is a simple quadratic algebraic equation with respect to  $a_{in}^*$ , and it has two solutions. Since over-saturation is not permitted, only the smaller solution is considered. Figure 4 depicts the schematic of open loop operation of the klystron. Since the model is not exact, the actual output amplitude,  $y$ , differs from  $y^*$ . Hence, a pulse-to-pulse feedback is needed to achieve the desired amplitude more precisely. The properties of the feedback are discussed in the following section.

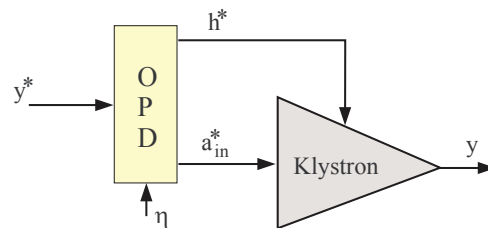


Figure 4: The schematic of open-loop operation of a klystron. The OPD-box denotes the operating point determination.

### PULSE-TO-PULSE FEEDBACK

The term “pulse-to-pulse” refers to the fact that the system runs in a pulsed mode and there is no intra pulse feedback to compensate the error. The closed loop diagram of the system is illustrated in Fig. 5. The controller is an integrator with the gain  $C$ . For slight changes of the setpoint, the high voltage remains constant and the desired amplitude is reached by

varying the headroom and thus the input amplitude,  $a_{in}^*$ . This threshold of the amplitude setpoint is determined by the allowed range of the klystron output, which is defined to be  $\pm\eta$  around the operating point (i.e. from the saturation level down to  $1 - 2\eta$  below the saturation, where  $\eta$  is the specified headroom). For the case where the setpoint change is beyond the threshold, a new set value for the high voltage power supply is determined with the default headroom,  $\eta$ , and the integrator resets, which leads to  $u = 0$ .

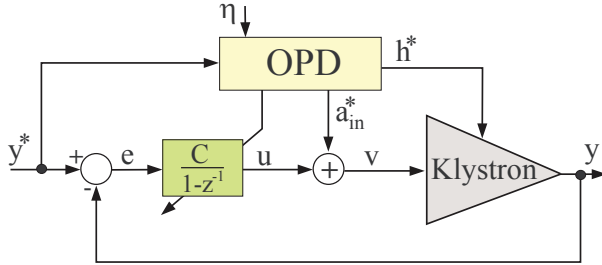


Figure 5: The schematic of closed loop operation of a klystron.

For the output  $y$ , we have the following expressions,

$$y_k = f(v_k, h^*) = f(a_{in}^* + u_k, h^*), \quad (6)$$

where  $f$  is model of the system response defined in (2), and where subscript  $k$  denotes the pulse index.

Approximating by Taylor's expansion implies,

$$y_k \approx f(a_{in}^*, h^*) + \left. \frac{\partial f(a_{in}, h^*)}{\partial a_{in}} \right|_{a_{in}=a_{in}^*} u_k, \quad (7)$$

For simplicity in notation, we define

$$f' := \left. \frac{\partial f(a_{in}, h^*)}{\partial a_{in}} \right|_{a_{in}=a_{in}^*} \text{ and } f_0 := f(a_{in}^*, h^*).$$

The controller signal,  $u_k$  is generated as follows,

$$\begin{aligned} u_k &= u_{k-1} + C(y^* - y_{k-1}) \\ &= u_{k-1} + C(y^* - f_0 - f' u_{k-1}), \end{aligned} \quad (8)$$

with a certain upper bound, to prevent excessive control-output and over-saturation of the klystron. In the case where the actuator hits the limit,  $a_{in}^*$  and  $h^*$  are recalculated for slightly larger headroom.

Substituting Eq. 8 into (7) leads to,

$$y_k = (1 - C f') y_{k-1} + f' C y^*. \quad (9)$$

Taking the term  $C f'$  constant and neglecting higher order terms in the Taylor series approximation, make the klystron system linear from the setpoint  $y^*$  to the output  $y$ . Notice that  $f'$  is a function of  $a_{in}^*$ , which itself is a function of  $y^*$ .

For fast transient response, the controller gain is chosen such that  $C = \frac{1}{f'}$ . However, in practice, the model is not exact, therefore the local gain of the actual system,  $g' = \frac{\partial y_k}{\partial a_{in}}$ , differs from  $f'$ . Thus, the system dynamics are,

$$y_k = (1 - \frac{g'}{f'}) y_{k-1} + \frac{g'}{f'} y^*. \quad (10)$$

To ensure the stability of the closed-loop [5], we have the following constraint,

$$\left| 1 - \frac{g'}{f'} \right| \leq \beta < 1, \quad (11)$$

which implies that the error decays at a rate of  $\beta^k$ .

The stability criterion in (11), leads to

$$\frac{1}{1 + \beta} < \frac{f'}{g'} < \frac{1}{1 - \beta}, \quad (12)$$

which indicates that the derivative of the model,  $f'$ , should be within a limit with respect to the true system.

## EXPERIMENTAL RESULTS

In the following experiment which is done on a klystron in a C-band RF station, different power setpoints are applied and the headroom is set to be  $\eta = 3\%$  from the saturation level.

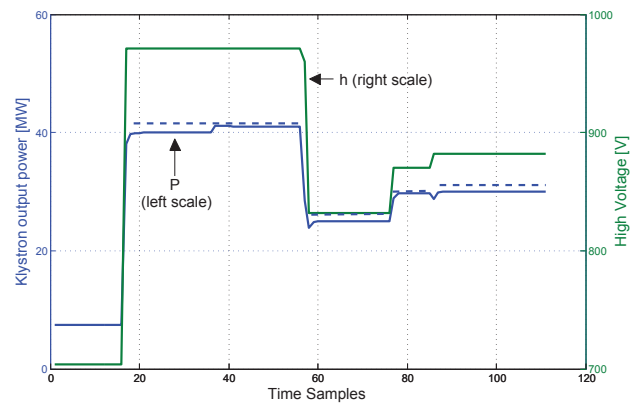


Figure 6: Closed-loop experiment result of applying different power setpoints. The high voltage power supply value is determined by the OPD unit and the pulse-to-pulse feedback gain,  $C$ , is modified accordingly. The dashed lines indicate the maximum power (saturation level).

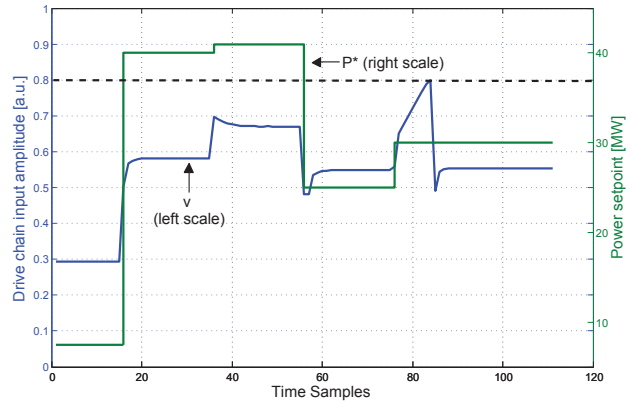


Figure 7: The input signal,  $v$ , to the klystron and the power setpoint,  $P^*$ . The dashed line denotes the maximum drive chain input.

Figure 6 illustrates the output power and high voltage power supply of the klystron for a series of step changes in the

setpoint. At time  $k = 16$  the setpoint jumps to  $P^* = 40\text{MW}$ . The OPD provides the new integrator gain,  $C$ , as well as the corresponding high voltage power supply set value for the modulator which is  $972\text{V}$ . The high voltage setting of the modulator responds relatively quickly, but it may take one or two pulses to reach the set value. During this time, the integrator value is set to zero and the feedback is still inactive. At time  $k = 36$  the setpoint is slightly increased by  $1\text{MW}$ . Since the new setpoint can be reached within the current headroom, the high voltage is kept unchanged and only the input amplitude is increased (by reducing the headroom to  $1\%$ ).

At time  $k = 56$ , the setpoint drops almost to half of the power,  $25\text{MW}$ , and the corresponding high voltage power supply value is set to  $832\text{V}$ . At time  $k = 76$ , the headroom is manually reduced to  $\eta = 1\%$  to observe the accuracy of modeling and the setpoint is set to  $30\text{MW}$ . Because of model-mismatch, and specifically due to the small headroom, the klystron saturates and the actuator signal,  $v$ , hits the limit of the drive chain input (see Fig. 7). In this case, the OPD unit is notified and the new operating point is determined with a new larger headroom. As we can see, at  $k = 85$  a new high voltage power supply set value is introduced with a new headroom (as default  $3\%$ ) and the output power has reached the setpoint of  $30\text{MW}$ .

## CONCLUSION

This paper has illustrated the klystron AM/AM modeling and its applicability in the model-based automation of a klystron. Using the klystron models also gives an opportunity to operators to monitor the operating point of klystrons, as well as the saturation levels. As a result of such automation, the open-loop drive chain from the vector modulator to the klystron output is linearized, and the closed-loop system reaches the setpoint more quickly. The minimum amount of headroom to the saturation is limited by the error between the models and the data as given in Fig. 2. A model-based pulse-to-pulse feedback is tested successfully on the Swiss-FEL full scale C-band RF system. The feedback approach is based on an integrator with an adaptive gain, depending on the setpoint.

## ACKNOWLEDGMENT

The authors would like to thank the LLRF and the RF team who made this research possible.

## REFERENCES

- [1] Romain Ganter et al., SwissFEL Conceptual Design Report, PSI, Villigen, Switzerland, 2010.
- [2] M. Omet et al., "Development and Test of Digital LLRF Control Procedures and Techniques in Scope of ILC", presented at the LLRF2013 workshop, Lake Tahoe, USA, October 1 - 4, 2013.
- [3] Ch. Rapp, "Effects of HPA-Nonlinearity on a 4-DPSK/OFDM-Signal for a Digital Sound Broadcasting System", *Proc. of 2nd European Conference on Satellite Communications*, Liege, Belgium., Oct. 1991, pp. 179–184.
- [4] A. J. Cann, "Nonlinearity Model With Variable Knee Sharpness", *IEEE Trans. Aerosp. Electron. Syst.* vol. 16, no. 6, pp. 874–877, Nov. 1980.
- [5] G.F. Franklin et al., *Digital Control of Dynamic Systems*, Addison Wesley, 1998.